Available online at www.sciencedirect.com
SCIENCE DIRECT
Journal of Molecular Catalysis B: Enzymatic 38 (2006) 139–147
JOURNAL OF MOLECULAR CATALYSIS B: ENZYMATIC
www.elsevier.com/locate/molcatb

Quantum mechanical study of *Burkholderia cepacia* lipase enantioselectivity

Sanja Tomić [a,*], Michael Ramek [b]

[a] *Institut Ruđer Bošković, Bijenička 54, HR-1000 Zagreb, Croatia*
[b] *Institute of Physical and Theoretical Chemistry, Graz University of Technology, Brockmanngasse 27/4, 8010 Graz, Austria*

Received 28 July 2005; received in revised form 17 November 2005; accepted 11 December 2005
Available online 18 January 2006

Abstract

Quantum mechanical, semiempirical (AM1) and ab initio (6-31G*) study of the *Burkholderia cepacia* lipase (BCL) catalysed reactions of the secondary alcohol esterification and its ester hydrolysis is presented. We have selected BCL for our study because of numerous experimental results available, but also because of its broad selectivity and stability that makes it interesting for industrial use. Previously we developed models for predicting lipase stereo-selectivity towards primary and secondary alcohols according to their structural parameters. In this work we show that not all of the experimentally determined binding modes are catalytically competent and that additional molecular modelling should be accomplished in order to find good starting points to study chemical reactions. The binding modes from which chemical modification of a substrate is possible are the most relevant for understanding enzyme selectivity and for the rational enzyme engineering.

We also investigated the influence of the tetrahedral atom type, C and P, upon the energy barriers in the proton transfer reactions from the catalytic histidine (His286) to either the catalytic serine (Ser87) or the alcohol oxygen of the substrate.

Keywords: Lipase catalysis proton transfer; Hydrolysis of secondary alcohol ester; Esterification of secondary alcohol; *Burkholderia cepacia* lipase; Quantum mechanical study; Molecular modelling

1. Introduction

Enzymes are important catalysts in the living organisms. Besides their importance in medicine and biology they are under the scope of scientists because of their application in biotechnology, as well. In this respect the most widely studied enzymes are those from microorganisms, especially microbial lipases since they are relatively easy available and promote a broad range of biocatalytic reactions. The natural function of lipase (glycerol ester hydrolases E.C. 3.1.1.3) is to catalyse ester bond hydrolyses of triglycerides, but they also very efficiently catalyse esterification, interesterification, alcoholysis, acidolysis, and aminolysis [1–5]. Especially important is their efficiency in the syntheses of enantiomerically pure products. Synthesis of only one enantiomer, instead of racemic mixtures, is a necessity in pharmaceutical industry because often only one enantiomer has the desired activity, whereas no activity or even undesirable side effects reside in the other enantiomer.

Our research has been concentrated on the lipase from *Burkholderia cepacia* (formerly *Pseudomonas cepacia*). There is a large amount of experimental data available for *Burkholderia cepacia* lipase (BCL): kinetic measurements [1,3–8], crystal structures of native enzyme and its complexes with the triglyceride like- and secondary alcohol ester like-inhibitors [9–13], but mechanism of its enantioselective catalysis is still not completely understood. Our theoretical research is aimed at understanding this mechanism. Previously we developed models for predicting lipase stereo-selectivity towards primary and secondary alcohols according to their structural parameters [14–17]. In this work we concentrate on the BCL active site and, using combined force field and quantum mechanical methods, study the proton transfer reactions. Study of these reactions, namely an alcohol esterification and an ester hydrolysis, is possible only if the orientation of a substrate in the active site is known. Determination of the correct orientation of an enantiomer in the active site is not a trivial task, and there is no consensus between the molecular modelling studies that have been accomplished. The X-ray structures

* Corresponding author. Tel.: +385 1 456 1025; fax: +385 1 468 0245.
E-mail address: sanja.tomic@irb.hr (S. Tomić).

1381-1177/$ – see front matter © 2005 Elsevier B.V. All rights reserved.
doi:10.1016/j.molcatb.2005.12.005

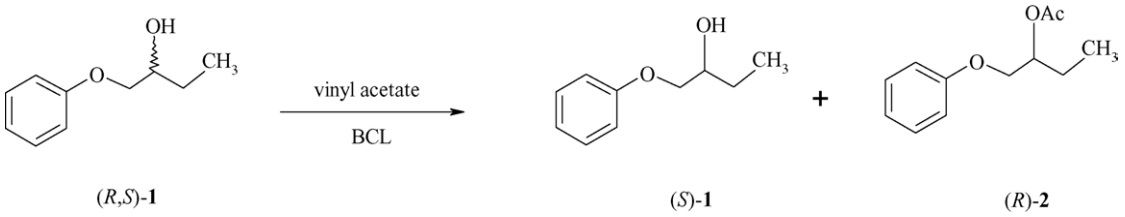

Scheme 1. BCL-catalysed enantioselective transesterification of 1-phenoxy-2-hydroxybutane (**1**). The product is1-phenoxy-2-acetoxybutane (**2**).

of transition state analogues bound to *Candida rugosa* lipase (CRL) suggested that two enantiomers bind in similar position, but with different orientation of alcohol oxygen and hydrogen at the chiral centre [18] (so called H/O permutation). A molecular modelling study performed by Zuegg et al. [19] for BCL and CRL suggested permutation of the large (L) and medium (M) substituents at the secondary alcohol chiral centre, and permutation of hydrogen and M at the primary alcohol chiral centre. They suggested that the L substituent of the primary alcohol binds at the hydrophobic pocket (HA) of the BCL active site. The theoretical study performed by Tomić et al. [20] for BCL with primary alcohols revealed that both enantiomers bind in similar orientations with the L accommodated into the hydrophilic pocket (HH) or pointing toward the entrance of the binding site. This is in accord with recently determined crystal structures of the transition states of BCL with two phosphonate analogues of the primary alcohol, 2-methyl-3-phenyl-1-propanol [21]. In these structures a similar binding of two enantiomers occurs, with the benzyl group of the alcohol pointing toward the solvent.

Although at first glance some of these results are contradictory, more than one might be correct. The orientation may differ for different lipases or even for different alcohols binding to the same lipase.

In our earlier investigations we were mainly focused on the secondary alcohols with an aryl ring, such as, for example, 1-phenoxy-2-hydroxybutane (**1** in Scheme 1) used in the present work as well. In this study we try to elucidate the importance of the tetrahedral intermediate in the secondary alcohol esterification catalysed by BCL, and to determine the most probable binding mode for the slow reacting enantiomer of **1**. Also we investigate the influence of the tetrahedral atom type, C and P, on the energy barriers in the proton transfer reactions, from the catalytic histidine (His286) to either the catalytic serine (Ser87) or the alcohol oxygen of the substrate.

Kinetic resolution of **1** revealed that BCL catalyses acetylation of *rac*-**1** with high enantioselectivity ($E > 200$), with the (*R*)-enantiomer being the reactive one [6,7]. Previously we found a few possible orientations of each enantiomer of **1** in the BCL active site. However, while the fast reacting enantiomer forms the proposed geometry of the tetrahedral intermediate [19] (TI, see Scheme 2) in several orientations, the slow reacting enantiomer forms the TI in only one orientation. The main idea of this study is to investigate the reaction possibilities of the slow and fast reacting enantiomer in different binding modes. It is assumed that formation of the substrate TI in the enzyme active site is necessary for the reaction to occur. However, the TI formed in the reactions catalysed by lipases is unstable, and the enzyme–inhibitor complexes, whose crystal structures are available, are often used to approximate it. In this work we try to rationalize possible pitfalls and accuracy of such an approach. In order to elucidate the process of the *Burkholderia cepacia* lipase-catalysed esterification of **1** we carried out a series of semiempirical (AM1) and ab initio calculations. The models used in this study have been derived either by force field based conformational searches [17] or determined by X-ray crystallography [13].

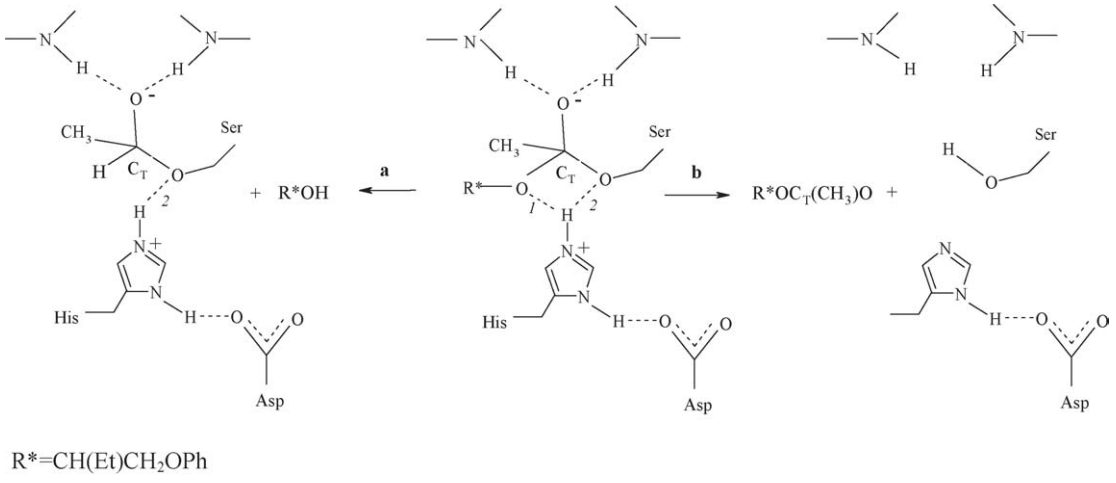

Scheme 2. The tetrahedral intermediate (TI) of **2** bound into the BCL active site (or in other words, TI of **1** bound to the acetylated BCL Ser87). The TI is defined by five hydrogen bonds important for the proton transfer and the substrate stabilisation, formed between the substrate and catalytic triad (Ser87, Asp264 and His286) and between the substrate and the protonated amide nitrogen of Leu17and Gln88 (members of the oxyanion hole). Numbers 1, and 2 are used to label the two possible proton transfer paths. Accompanied reactions are hydrolysis (a) and esterification (b), leading to release of **1** and **2**, respectively.

2. Methods

2.1. Force field

For our study of BCL-catalysed esterification of the secondary alcohol and its ester hydrolysis we modelled covalent and non-covalent complexes between BCL with acetylated Ser87, i.e. serine belonging to the catalytical triad, and *R* and *S* enantiomers of 1-phenoxy-2-hydroxybutane. For this purpose we used the crystal structure of the complex of BCL with the phosphate analogue of 1-phenoxy-2-acetoxybutane (Protein Data Bank code 1HQD). The bound substrates were built using the inhibitor in 1HQD as a template in which the $P(CH_3)O^-$ group covalently bound to Ser87, was replaced by the $C(CH_3)O^-$ group. Hydrogens were added, to correspond to pH 7.0, histidines were uncharged (mono-protonated), aspartic and glutamic acids were negatively charged, and arginines and lysines were positively charged. According to the assumed reaction path the catalytic His286 was doubly protonated in the case of covalent complex, and neutral with hydrogen at Nδ in the case of non-covalent complex. Parameterisation was performed in the all atom AMBER force field [22] (for details of the parameterisation see our previous works [16,17].

All water molecules found in the BCL–inhibitor complex 1HQD, (altogether 291 molecules), were included in the molecular modelling procedure, while the bulk water influence was modelled by a distance dependent dielectric constant.

We consider two different orientations for each enantiomer covalently bound in the BCL active site (*R* is the fast reacting and *S* is the slow reacting enantiomer). One orientation is equivalent to the orientation of the secondary-alcohol-like inhibitor in the crystal structure (R_c and S_c), and the other represents the conformation determined by molecular modelling, R_m and S_m. They were determined as the lowest energy BCL-(*R*)-**1** and (*S*)-**1** complexes, independently by the Monte Carlo Multiple Minimum (MCMM) [23] and Low Mode Conformational Search (LMCS) [24] as implemented in the program MacroModel.

While R_c and S_c orientations are practically identical, see Fig. 1, the orientations R_m and S_m significantly differ (Fig. 2).

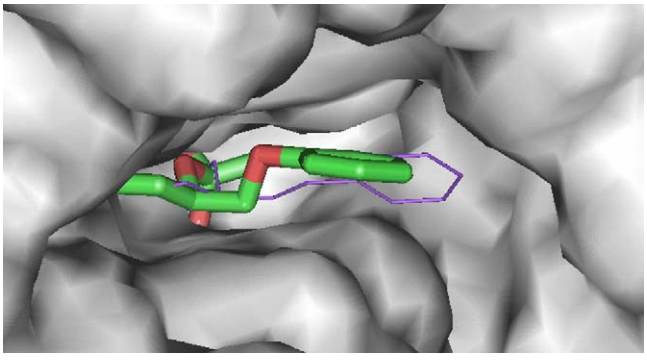

Fig. 1. Superposition of R_c (thick) and S_c (thin-violet) binding modes of **1**. This is a view from the entrance to the active site bottom (Ser87) with His286 situated above the substrate. (For interpretation of the references to colour in this figure legend, the reader is referred to the web version of the article.)

According to our previous study [13], the tetrahedral C atom of the acetyl group is in its *S* configuration.

Both binding modes R_c, R_m, and S_m have the proposed geometry of the reaction intermediate, the tetrahedral intermediate (TI) as displayed at Scheme 2, i.e. they have five hydrogen bonds important for the substrate stabilisation and the proton transfer: Oδ2(Asp264)···Hδ1(His286), Hε(His286)···Oγ(Ser87), Hε(His286)···O(alcohol), and hydrogen bonds between oxyanion (O^-) and protonated amide nitrogens of Leu17 and Gln88 (see Scheme 2). In the S_c binding mode the Hε(His286)···O(alcohol) hydrogen bond is missing, i.e. it does not have geometry of the proposed tetrahedral intermediate.

2.2. Semiempirical calculations

For the purpose of semiempirical calculations we prepared a model consisting of 22-amino acid residues and the substrate, starting from the optimised protein–substrate complex. Besides substrate, the model comprises the amino acid residues that enclose the BCL binding site: Leu17, Thr18, Tyr23, Tyr29, His86, Ser87, Gln88, Phe119, Ala120, Val123, Leu164, Leu167, Ser244, Ala247, Leu248, Thr251, Val266, His286, Leu287, Ile290, Asn292, and Leu293. The surface of amino acid residues in the reduced model is shown in Fig. 2. Since His286 is positively, and oxyanion negatively charged, the overall system is neutral.

The four different binding modes, R_c, R_m, S_c, and S_m were energy optimised using the AM1 procedure [25] in the programs MOPAC2002 [26] and GAMESS [27]. During the optimisation, the backbone atoms of the amino acid residues were fixed in order to preserve the active site shape. In each binding mode, both reactions, hydrolysis of **2** and esterification of **1**, were studied. To set up the input for the MOPAC202 calculations we used the program Triton [28]. MOPAC calculations were used to perform a scan search, while GAMESS calculations were

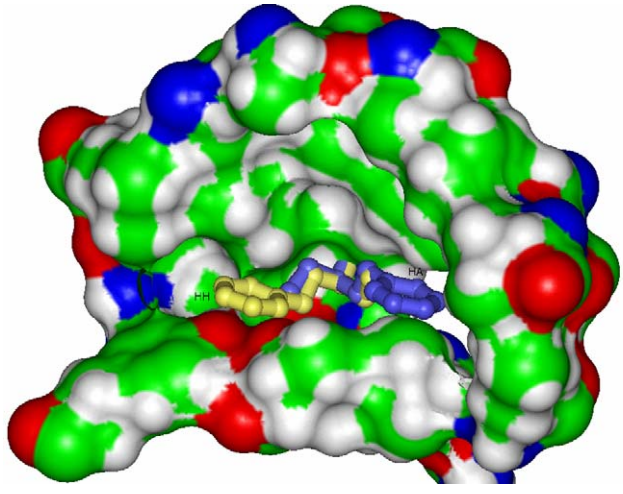

Fig. 2. Superposition of R_m (violet) and S_m (yellow) binding modes of **1**. HA is the hydrophobic, and HH partly hydrophilic pocket in the BCL active site. The surface of the amino acid residues used in semiempirical calculation is displayed. (For interpretation of the references to colour in this figure legend, the reader is referred to the web version of the article.)

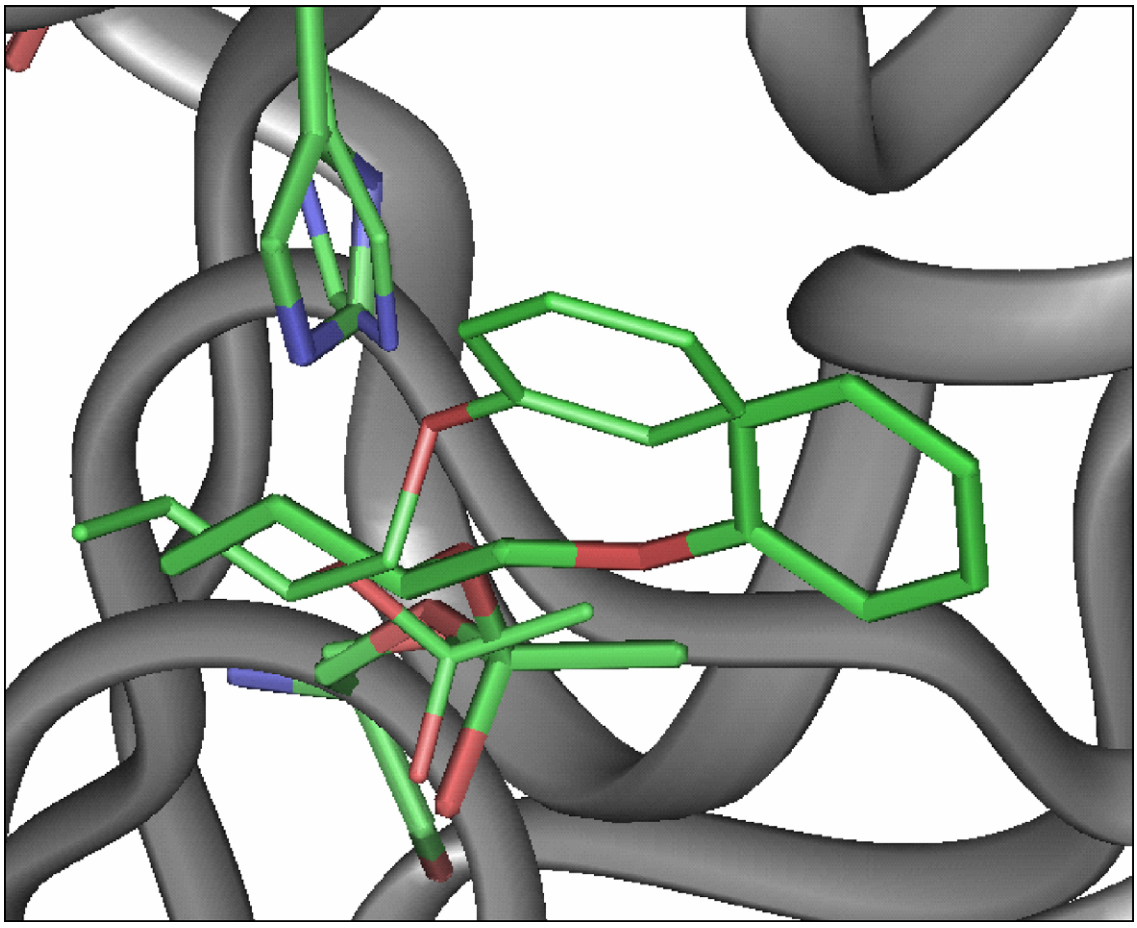

Fig. 3. Superposition of R_c (thick) and R_m (thin) binding modes of **1**.

used in an attempt to locate the most interesting transition states directly.

To model hydrolysis, we defined a reaction coordinate made up of the distances between the alcohol O atom and the Hε atom of His286, and between the same O atom and the tetrahedral carbon atom C_T of the TI acetyl group. In the hydrolysis reaction, the H atom moves from His286 to the alcohol oxygen and the covalent bond between the alcohol oxygen and C_T is elongated until it breaks. The unbound alcohol is then released (Scheme 2).

For the esterification, we defined similar reaction coordinate from the distance between Oγ of Ser87 and Hε of His286, and the distance between the same O atom and the tetrahedral carbon atom C_T. During the esterification, the H atom is transferred from His286 to Oγ, and the bond between Oγ and C_T breaks. Finally the ester **2** (Scheme 2) is released.

For both reaction pathways the O–H bond formation was adjusted discretely while the fragmenting C–O bond was allowed to relax to its optimum value. During the investigation of the reactions, optimisation of the models by AM1 revealed changes in side chain orientation for His86, Val123, Leu248 and His286. This is partly due to the missing protein environment. To avoid unnatural orientations of the amino acid side chains during the reactions, the protein part was fixed, while substrate (acetyl-alcohol) and Hε at His286 were free to move.

2.3. Ab initio calculations

To complete the theoretical picture, we also performed ab initio RHF calculations to get a first principle estimate of energy differences and barriers. For these calculations we prepared a further simplified model, which we extracted from the 22-amino acid models optimised by AM1. It consisted of only two-amino acid residues, namely His286 and Ser87, and the substrate, adding up to a total of 63 atoms. The overall system was neutral ($His286^+$, O^-). Energies of these systems were calculated using the programme GAMESS [27] and the 6-31G* basis set. During the optimisation, only hydrogen atoms were free to move.

3. Results and discussion

A number of theoretical studies have been performed in order to understand the molecular basis of lipase selectivity. One approach, e.g., is to model the average covalent enzyme–substrate complexes [29–32] using MD simulations, and to correlate the enantioselectivity with the selected geometrical values, like the $H_{N\varepsilon}$–$O_{alcohol}$ distance [29] or the position of the catalytic histidine [31]. The most common strategy, however, is to model the tetrahedral intermediate (TI), covalent substrate–enzyme complexes, that represent local minima on

Table 1
Relative energies (kcal/mol) of different binding modes determined by molecular mechanics [13], semiempirical AM1, and 6-31G* RHF ab initio calculations

Binding mode	ΔE (AMBER)	ΔE (AM1)	ΔE (ab initio)	H–$O_{alcohol}$	H–Oγ
R_c	0.2	30	41	3.23	2.93
R_m	0	0	0	2.83	3.01
S_c	4.1	32	78	3.99	2.75
S_m	2.2	19	24	2.87	2.98

The left column refers to the complete protein with the crystal waters included, the middle one to the 22-amino acid model, and the last column to the two-amino acid model. In the last two columns distances between the His286 Nε hydrogen and substrate and serine oxygen, $O_{alcohol}$ and Oγ, respectively are given. R_m and S_m are determined by the molecular modelling and R_c and S_c are the optimised crystal structures.

Table 2
The results of the secondary alcohol **1** esterification modelled by AM1 in MOPAC202

Binding mode	ΔE (TS[a]–IS[b])	ΔE (TS–FS[c])	Oγ···C_T (Å)	Oγ–H (Å)
R_c	25	61	2.90	0.96
R_m	25	62	2.81	1.00
S_c	15 (6)	59	2.86	1.00
S_m	26 (15)	64	2.85	1.00

In the columns on the left the energy barriers (kcal/mol) for the ester release and for its binding are given. The values in parenthesis are determined by the transition state searching method. The last two columns comprise the final values of the bond lengths relevant for the reaction coordinate (product).
[a] Transition state.
[b] Initial state (covalent complex).
[c] Final state (non-covalent complex).

the substrate transformation potential energy hyper surfaces. Molecular modelling and the X-ray structure of the phosphonate analogue of the *R*-**1** [13] support the tetrahedral intermediate in Scheme 2 as the intermediate in lipase-catalysed esterification and hydrolysis. However, the X-ray structure of the phosphonate analogue of the *S*-**1** [33] does not resemble the proposed TI topology and, in order to locate a good initial point from which to model the chemical transformation of *S*-**1**, additional molecular modelling, conformational search, is needed. Our previous study [15,17] resulted in different binding modes of the two enantiomers of **1** in the lipase active site. Further more, for the fast reacting enantiomer, it revealed a few different binding orientations. The most buried one, R_c binding, is close to the experimentally determined binding mode of the inhibitor analogue of the secondary alcohol ester (Fig. 1). In this orientation the phenyl ring (part of the large substituent, Ph–O–CH_2) is situated in the large hydrophobic pocket, HA. By looking into the active site with Ser87 at the bottom and His286 situated above the substrate, HA is on the right, and HH on the left side of His286. In the other binding modes, the phenyl ring is less buried and in the lowest energy form (R_m) the phenyl ring points to the entrance of the active site funnel (Fig. 3).

For the slow reacting enantiomer, molecular modelling indicates only one low energy orientation in which the tetrahedral intermediate is formed, S_m (Fig. 2). The orientations of the L and M substituents in this binding mode are opposite to their orientation in the experimentally determined S_c mode (equivalent to the R_c mode, Fig. 1), namely the phenyl ring is mostly buried inside the partly hydrophilic, HH pocket. The current study does not exclude the possibility of S_c binding, but finds it unsuitable for developing the tetrahedral intermediate. While the X-ray structure of the BCL complex with the fast reacting secondary alcohol like inhibitor can be used as an approximation of the stable intermediate (TI, at Scheme 2), this is not the case with the X-ray structure of the BCL complex with the slow reacting secondary alcohol like inhibitor.

According to the semiempirical AM1 calculations, and in agreement with our molecular modelling results, the lowest energy binding mode is R_m. In the order of increasing energy, the binding modes S_m, R_c and S_c follow in this sequence (Table 1).

Table 3
The results of the ester (**2**) hydrolysis modelled by AM1 in MOPAC202

Binding mode	ΔE (TS[a]–IS[b])	ΔE (TS–FS[c])	$O_{alcohol}$···C_T (Å)	$O_{alcohol}$–H (Å)
R_c	68	48	2.90	0.98
R_m	40	54	2.90	0.95
S_c	88 (∞)	68	2.62	0.96
S_m	41 (19)	38	2.83	0.99

In the columns on left the energy barriers (kcal/mol) obtained for the alcohol release and for its binding are given. The values in parenthesis are determined by the transition state searching method. The last two columns comprise the final values of the bond lengths relevant for the reaction coordinate (product).
[a] Transition state.
[b] Initial state (covalent complex).
[c] Final state (non-covalent complex).

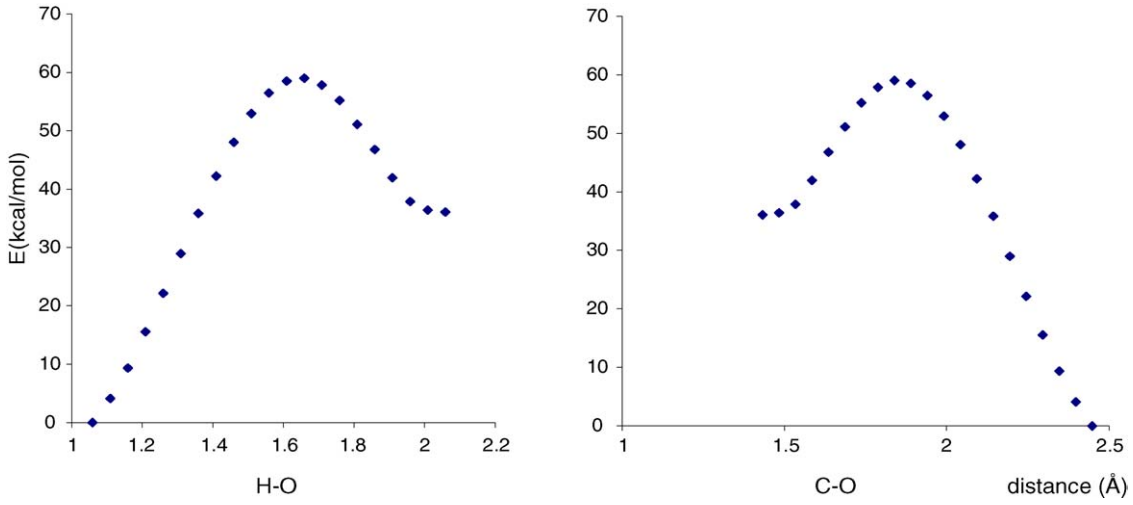

Fig. 4. AM1 energy profile (kcal/mol) for esterification of the *R*-**1** starting from the R_m binding mode using the scan method, as a function of distances (Å) between Ser87:Oγ and His286:$H_{N\varepsilon}$ (left), and between Ser87:Oγ and C_T (right). The reaction starts at E_{rel} = 38 kcal/mol.

The same ordering is determined by the (6-31G*) ab initio calculations on the further reduced systems consisting of only His286, Ser87 and the substrate (see Section 2). Energy differences between the binding modes increase with decreasing size of the system. The bigger system can more easily compensate some locally unfavourable interactions, which are most pronounced in the S_c binding mode. Haeffner et al. [34] noticed the same trend using the energy based subsets in the molecular mechanics approach.

The results for the esterification of **1**, and for the hydrolysis of **2**, modelled by the AM1 are summarised in Tables 2 and 3, respectively. The initial state is the covalent enzyme–substrate complex (Table 1). In the case of R_c, R_m and S_m this is a proposed TI (Scheme 2). We should stress that the calculated relative energies are only a very crude approximation of the real values, which is already obvious by comparing the relative energies of the binding modes calculated on systems of different complexity by different methods (Table 1). However, since the same approximations are used for all the binding modes, we can argue that the calculated values can be used to extract qualitative conclusions about binding of the two enantiomers in the lipase active site.

Both reactions, ester formation and hydrolysis start from the same either experimentally (R_c and S_c) or theoretically determined (R_m and S_m) covalent substrate–enzyme complex (see Table 1). During the ester formation hydrogen is from His286 transferred to serine oxygen Oγ. During the hydrolysis hydrogen is from His286 transferred to the alcohol oxygen.

The barriers for the ester formation are similar for both modes of the fast reacting enantiomer, R_m and R_c (Table 2, Figs. 4 and 5). The reaction of hydrolysis is more easily accomplished from the R_m binding mode (Table 3). However, since according to the molecular dynamic results [17], a transition between R_m and R_c is easily feasible at room temperature, we can conclude that the secondary alcohol **1** bound in any of them will be transformed to the ester.

The results for the slow reacting enantiomer are different, the barrier for the alcohol formation is much lower in the S_m (Fig. 6) than in the S_c mode, but for the ester formation it is lower in the S_c binding mode (Tables 3 and 2, respectively). Because of the high barrier for the reaction of hydrolysis in the S_c binding mode and since it is hard to accomplish reorientation from S_c to S_m, we can conclude that the ester bound in the S_c orientation will be most probably released unchanged.

In order to investigate the reactions of the slow reacting enantiomer beyond the simple grid method, we also performed transition point searches. These searches revealed an even lower barrier for the ester formation in the S_c binding mode of 6 kcal/mol, but the reaction of hydrolysis from this binding mode was found to be impossible. The H moving from Nε of His286 to the alcohol oxygen soon turned into the energetically more favourable direction towards Oγ, thus leading to esterification. For S_m, these transition state searches yielded the following barriers: 19 kcal/mol for the

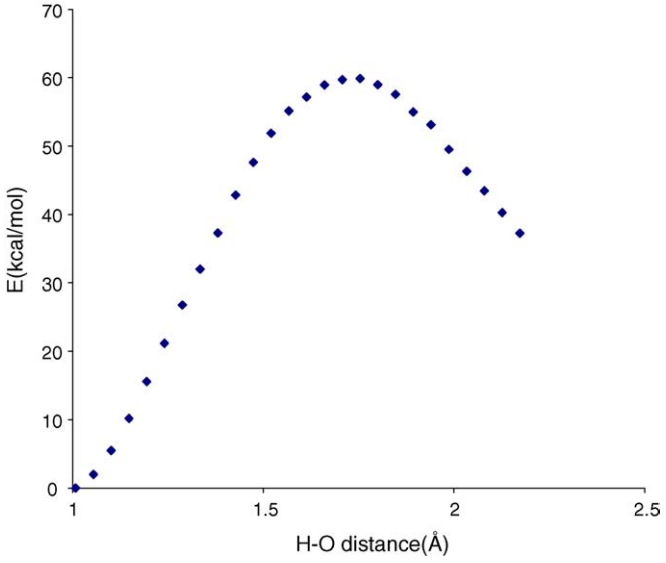

Fig. 5. AM1 energy profile (kcal/mol) for esterification of the *R*-**1** starting from the R_c binding mode obtained by scan, as a function of the distance (Å) between Ser87:Oγ and His286:$H_{N\varepsilon}$. The reaction starting point is the first on the right.

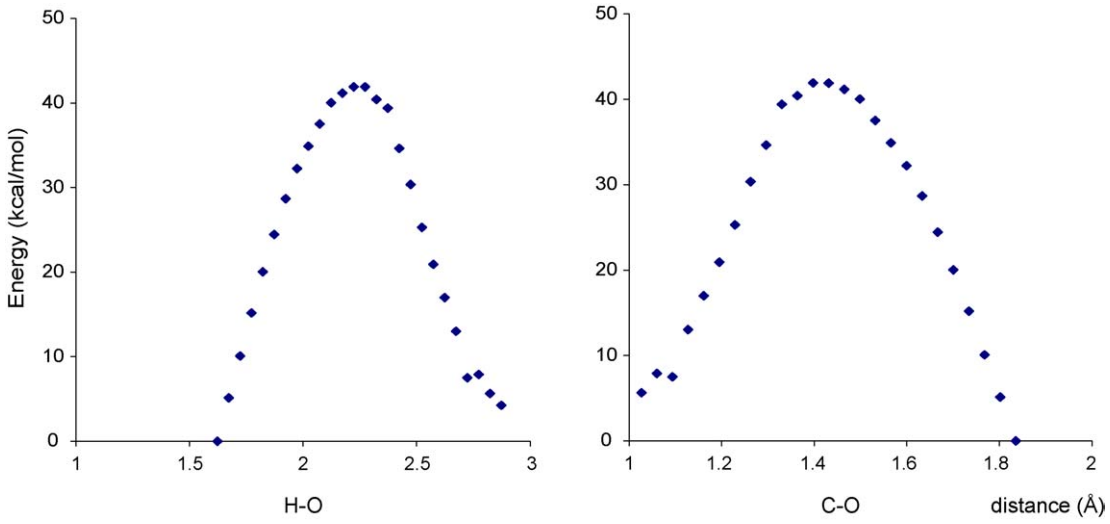

Fig. 6. AM1 energy profile (kcal/mol) for hydrolysis of the *S*-**2** starting from the S_m binding mode using the scan method, as a function of distances (Å) between $O_{alcohol}$ and His286:$H_{N\varepsilon}$ (left) and between $O_{alcohol}$ and the acetyl C_T (right). The reaction starts at E_{rel} = 4 kcal/mol.

ester formation and 15 kcal/mol for the alcohol formation (see Tables 2 and 3).

To study the whole process, either an ester hydrolysis or an alcohol esterification, the following series of steps should be considered. For an ester hydrolysis: entrance of the ester into the BCL binding site, covalent complex formation, release of the alcohol. For an alcohol esterification: acylation of the enzyme (e.g. binding of acetyl to Ser87), entrance of an alcohol into the BCL active site, covalent complex formation, release of the ester. If we consider binding of an alcohol and its ester to BCL (i.e. formation of non-covalent complexes) to be of equal probability, than we can argue that these two reactions should not differ. However, the covalent complex formation and the substrate release, should be considered together as the rate determining events. In this work we modelled only the covalent complexes collapse, i.e. substrate, either alcohol or ester release. However, the reaction of the ester hydrolysis is the reverse to the covalent binding of the alcohol to the acetylated Ser87 of the BCL and the energy difference between the final and transition states gives us an idea about the propensity for the secondary alcohol and acetylated enzyme system to transform from the non-covalent to the covalent complex (Table 3, Fig. 6). Similarly, the reaction of alcohol esterification provides hints about transformation of the non-covalent enzyme–ester complex to the covalent one (Table 2, Fig. 4). The energy barriers for binding of the fast reacting enantiomer of both alcohol and ester are similar for the R_m and R_c binding modes. In both of these modes the tetrahedral intermediate is formed, and the reactions can take place. In the case of the slow reacting enantiomer the barriers for both, ester binding and release are lower for the S_c than for the S_m binding mode. Since the S_c binding mode is not a proposed TI, the energy barrier for the reaction of hydrolysis calculated by the simple scan method is very high.

To summarise, the fast enantiomers, *R*-**1** and *R*-**2** bind into the BCL active site in a few different orientations with similar probability. Since all of these orientations lead to the reaction and finally the release of the product, we call them 'productive binding modes'. The slow enantiomer, *S*-**2** can also bind in two different binding modes. The energy difference between the covalent complexes of BCL and *S*-**2** bound in these two orientations is small with S_m being more favourable. According to the modelled reactions, hydrolysis can be easily accomplished from this, but not from the S_c binding mode. The ester that binds to BCL in the S_c orientation most probably will be released unchanged. These results are in agreement with the study of Nakamura and Tekenaka [35], who found that in the case of *Pseudomonas* sp. lipase-catalysed hydrolyses of benzoate esters with bulky substituents at the alcohol chiral centre addition of catechines improves the enantioselectivity. Binding of catechins in the partly hydrophylic, HH, pocket unables the slow reacting enantiomer to accomodate the productive, 'm', orientation. In this way, the conversion rate is decreased, but the enantioselectivity is increased. In the free protein and in its complex with the phosphonate analogue of **2** there are water molecules bound in the HH pocket that have to be expelled from it in order to enable S_m binding of the slow enantiomer; hence to estimate a binding mode probability the protein disolvation should also be included. S_c appears to be a convenient way for the inhibitor, an analogue of the slow reacting enantiomer of the ester **2** to bind to the enzyme, but cannot be used as a starting point to study hydrolysis of the substrate.

This study showed that the experimentally determined binding mode of the slow reacting enantiomer might be used to explain and predict enantioselectivity, either by considering the large distance between its alcohol oxygen and the His286:$H_{N\varepsilon}$ or the high barrier for the proton transfer. However, for rationalize enzyme engineering the all possible binding modes should be considered with highest weight on the productive ones.

3.1. H transfer ab initio study

The design of enzyme inhibitors as structural analogues of intermediates is well established. The analogue design paradigm

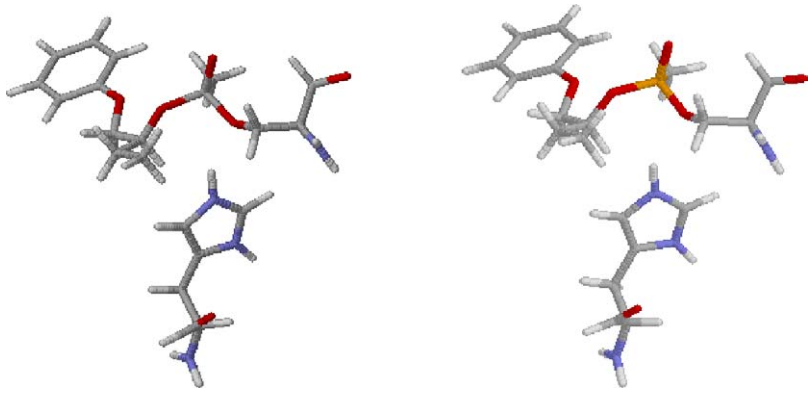

Fig. 7. Reduced, two-amino acid model of the S_c binding mode (left) and its phosphate analogue (right).

is based on replacing the central substrate functional group in order to unable reaction. By substitution of the tetrahedral carbon, C_T, by phosphorous, a scissile C–O bond is transformed to a non-scissile, P–O bond. Using RHF/6-31G* ab initio calculations we examined influence of the tetrahedral atom on the proton transfer barriers. Using the two-amino acid models we determined relative energies for the proton transfer from Nε of His286 to Ser87 oxygen and to the oxygen of the covalently bound substrate in two cases: with the substrate being (a) the secondary alcohol ester **2**, and (b) its phosphate analogue, lipase inhibitor (Fig. 7).

The results indicate that the replacement of the tetrahedral C atom with P significantly increases the barriers for the proton transfer (Table 4). In all cases the proton transfer barrier is 5–10 times higher for the inhibitor than the substrate. Shokhen and Albeck [36] performed a series of quantum mechanical ab initio calculations to determine stability factors that discriminate inhibitors from substrate of serine protease. They found that the strength of the new covalent bond between the enzyme and a ligand is the main source of the huge differences in the stability of covalent tetrahedral complexes formed by substrate and its transition state analogue inhibitor. According to our findings another reason for the large apparent stability of the (1-phenoxybut-2-yl)-methylphosphonate–BCL complex is the high barrier for the proton transfer.

In the similar manner to the AM1 semiempirical results, the hydrogen from Nε of His286 is more easily transferred to the alcohol oxygen of **1** in the S_m than in the S_c binding mode. In contrast, the same protein is more easily transferred to the oxygen of catalytic serine (Ser87) in the S_c binding mode.

Table 4
The energy barriers for the proton (Hε) transfer from His286 to Oγ of Ser87 and to substrate $O_{alcohol}$ (kcal/mol) obtained by ab initio calculation for the reduced, two-amino acid model of the S_c and S_m binding modes of **2** and its P-analogue (C_T replaced by P)

	S_c-inhibitor	S_m-inhibitor	S_c-substrate	S_m-substrate
H shifted to Oγ	45.9	92.5	4.8	16.4
H shifted to O_{alc}	45.9	37.0	9.3	0.5

4. Conclusion

The main purpose of this work was to elucidate which of theoretically and experimentally determined binding modes are appropriate to be considered as starting points in modelling chemical reactions, and to rationalize the reasons for high enantioselectivity of BCL towards **1**.

Force field based and quantum mechanical calculations were performed for the covalently bound ester **2** in the BCL active site. Both types of calculation indicated that the complex with the fast reacting enantiomer has lower energy than the one with the slow reacting enantiomer. However, the enthalpy difference is not the only reason for high enantioselection. The number of the catalytically competent binding modes for the fast enantiomer is significantly larger than for the slow enantiomer, hence the entropy difference should not be neglected.

According to the quantum mechanical calculations each of two different binding modes of the fast enantiomer, R_m and R_c (proposed by molecular modelling and X-ray diffraction, respectively) is catalytically competent. Differently, the experimentally proposed binding mode for the slow enantiomer, S_c is not catalytically competent. Apparently, the experimentally determined structure of an enzyme–inhibitor complex should be taken with caution, since it might not be appropriate starting points for the chemical reactions. For rational enzyme engineering and/or a substrate modification, it is necessary that all possible binding modes are considered, with the highest weight on those resembling the tetrahedral intermediate geometry.

Acknowledgements

This work was supported by grant 0098036 from the Ministry of Science and Technology of Croatia and the Austrian Academic Exchange Service (ÖAD project WTZ 15/2004). It is part of the bilateral collaboration between Republic Austria and Croatia. We are thankful Marija Luić and David Smith for critical reading the manuscript.

References

[1] R.J. Kazlauskas, U.T. Bornscheuer, in: H.J. Rehm, G. Reed, A. Pühler, P.J.W. Stadler, D.R. Kelly (Eds.), Biotransformations with Lipases in

Biotechnology, vol. 8, VCH Publishers, Weinheim, Germany, 1998, pp. 37–191.
[2] S.M. Roberts, J. Chem. Soc., Perkin Trans. 1 (2000) 611–633.
[3] R.D. Schmid, R. Verger, Angew. Chem. Int. Ed. Engl. 37 (1998) 1608–1633.
[4] K. Faber, Biotransformations in Organic Chemistry, 3rd ed., Springer, Berlin, 1997.
[5] K. Laumen, M.P. Schneider, J. Chem. Soc., Chem. Commun. (1988) 598–600.
[6] E. Ljubović, V. Šunjić, Croat. Chem. Acta 71 (1998) 99–117.
[7] E. Ljubović, V. Šunjić, Tetrahedron Lett. 41 (2000) 9135–9138.
[8] R.J. Kazalauskas, A.N.E. Weissfloch, A.T. Rappaport, L.A. Cuccia, J. Org. Chem. 56 (1991) 2656–2665.
[9] W.V. Tuomi, R.J. Kazlauskas, J. Org. Chem. 64 (1999) 2638–2647.
[10] J.D. Schrag, Y. Li, M. Cygler, D. Lang, T. Burgdorf, H.J. Hecht, R. Schmid, D. Schomburg, T. Rydel, J.D. Oliver, L.C. Strickland, C.M. Dunaway, S.B. Larson, J. Day, A. McPherson, Structure 5 (1997) 187–202.
[11] K.K. Kim, H.K. Song, D.H. Shin, K.Y. Hwang, S.W. Suh, Structure 5 (1997) 173–185.
[12] D.A. Lang, M.L.M. Mannesse, G.H. De Haas, H.M. Verheij, B.W. Dijkstra, Eur. J. Biochem. 254 (1998) 333–340.
[13] M. Luić, S. Tomić, I. Leščić, E. Ljubović, D. Šepac, V. Šunjić, L.J. Vitale, W. Saenger, B. Kojić-Prodić, Eur. J. Biochem. 268 (2001) 3964–3973.
[14] S. Tomić, M. Luić, D. Šepac, I. Leščić, E. Ljubović, B. Kojić-Prodić, V. Šunjić, in: H.-D. Holtje, W. Sippl (Eds.), Rational Approaches to Drug Design: 13th European Symposium on Quantitative Structure–Activity Relationships, Prous Science S.A., Barcelona, 2001, pp. 69–73.
[15] S. Tomić, B. Kojić-Prodić, J. Mol. Graph. Model. 21 (2002) 241–252.
[16] S. Tomić, Designing Drugs and Crop Protectants: Processes Problems and Solutions, Blackwell Publishing Ltd., Oxford, UK, 2003, pp. 326–328.
[17] S. Tomić, B. Bertoša, B. Kojić-Prodić, I. Kolosvary, Tetrahedron: Asymmetry 15 (2004) 1163–1172.
[18] M. Cygler, P. Grochulski, R.J. Kazlauskas, J.D. Schrag, F. Boutadded, B. Rubin, A.N. Serreqi, A.K. Gupta, J. Am. Chem. Soc. 116 (1994) 3180–3186.
[19] J. Zuegg, H. Hönig, J.D. Schrag, M. Cygler, J. Mol. Catal. B: Enzym. 3 (1997) 83–98.
[20] S. Tomić, V. Dobovičnik, V. Šunjić, B. Kojić-Prodić, Croat. Chem. Acta 74 (2001) 343–357.
[21] A. Mezzetti, J.D. Schrag, C.S. Cheong, R.J. Kazlauskas, Chem. Biol. 12 (2005) 427–437.
[22] W.D. Cornell, P. Cieplak, C.I. Payly, I.R. Gould, K.M. Merz, D.M. Ferguson, D.C. Spellmeyer, T. Fox, J.W. Caldwell, P.A. Kollman, J. Am. Chem. Soc. 117 (1995) 5179–5197.
[23] G.M. Keserű, I. Kolossváry, B. Bertók, J. Am. Chem. Soc. 119 (1997) 5126.
[24] I. Kolossvary, W.C.J. Guida, J. Comput. Chem. 20 (1999) 1671–1684.
[25] M.J.S. Dewar, E.G. Zoebisch, E.F. Healy, J.J.P. Stewart, J. Am. Chem. Soc. 7 (1985) 3902–3909.
[26] J.J.P. Stewart, MOPAC, Fujitsu Limited, Tokyo, Japan, 2002.
[27] M.W. Schmidt, K.K. Baldridge, J.A. Boatz, S.T. Elbert, M.S. Gordon, J.H. Jensen, S. Koseki, N. Matsunaga, K.A. Nguyen, S.J. Su, T.L. Windus, M. Dupuis, J.A. Montgomery, J. Comput. Chem. 14 (1993) 1347–1363.
[28] J. Damborský, M. Prokop, J. Koča, Trends Biochem. Sci. 26 (2001) 71–73.
[29] T. Schulz, J. Pleiss, R.D. Schmid, Protein Sci. 9 (2000) 1053–1062.
[30] J. Zuegg, H. Hönig, J.D. Schrag, M. Cygler, J. Mol. Catal. B: Enzym. 3 (1997) 83–98.
[31] B.-Y. Hwang, H. Scheib, J. Pleiss, B.-G. Kim, R.D. Schmid, J. Mol. Catal. B: Enzym. 10 (2000) 223–231.
[32] D. Guieysse, C. Salagnad, P. Monsan, M. Remaud-Simeon, V. Tran, Tetrahedron: Asymmetry 14 (2003) 1807–1817.
[33] M. Luić, private communication.
[34] F. Haeffner, T. Norin, K. Hult, Biophys. J. 74 (1998) 1251–1262.
[35] K. Nakamura, K. Tekenaka, Tetrahedron: Asymmetry 13 (2002) 415–422.
[36] M. Shokhen, A. Albeck, Proteins: Struct. Funct. Genet. 40 (2000) 154–167.